

Growth and Deformation Defects in Phyllosilicates as Seen by HRTEM

BY M. AMOURIC

Centre de Recherche sur les Mécanismes de la Croissance Cristalline, CRMC2-CNRS, Campus Luminy, case 913, 13288 Marseille CEDEX 09, France

(Received 6 January 1986; accepted 29 July 1986)

Abstract

High-resolution transmission electron microscopy (HRTEM) reveals a wide variety of deviations from perfect crystalline periodicity within many mineral groups. Among the defects, the linear and planar ones are particularly abundant in synthetic and natural phyllosilicates which show a quasi-one-dimensional structural organization. Directly related to the layer-by-layer or spiral growth stage, various dislocations and stacking faults are observed. They may explain, for example, the complex polytypic behaviour of micas and chlorite. In the same manner, specific deformation defects are easily visible. They characterize different degrees of deformation in phyllosilicates related to the tectonic history of their host rocks. Furthermore, HRTEM reveals that intercalations of different structural units may also occur in sheet silicates, accompanying their growth and deformation mechanisms. In this case, more or less important chemical changes are involved in addition to the structural changes, with all the consequences this may induce concerning the meaning and development of such 'mixed minerals'.

1. Introduction

It is their tri-periodic organization and their remarkable repeating geometry which characterize most crystal structures. However, crystals very often contain deviations from perfect periodicity. These defects are very interesting because they may give information on the origins and geological histories of minerals.

The impact of high-resolution transmission electron microscopy (HRTEM) on structural mineralogy is particularly impressive, but the most valuable capability of HRTEM concerns the study of defects (periodic or not) in minerals. Indeed, it generally permits the direct imaging of local regions of anomalous and defective structures (for example, superstructures and polytypes, stacking-fault nature and distribution, intimate structures of dislocation cores, microtwins, antiphases, non-stoichiometric microstructure relationships, etc.). In this respect, HRTEM is a very interesting method for completing X-ray diffraction studies on the structure of minerals.

Table 1. *Mica synthesis conditions and origins of the natural phyllosilicates studied*

(I) Synthetic specimens

Ph.: synthetic phengite. $T = 773$ K; $P_{\text{H}_2\text{O}} = 10^8$ Pa; $t = 168$ h; $\text{K}_2\text{CO}_3 + \text{MgO} + \gamma\text{-Al}_2\text{O}_3 + \text{SiO}_2$

Ms. 1: synthetic muscovite. $T = 893$ K; $P_{\text{H}_2\text{O}} = 10^8$ Pa; $t = 143$ h; stoichiometric mixture: $\text{K}_2\text{SO}_4 + \text{synthetic kaolinite } [\text{Al}_2\text{Si}_2\text{O}_5(\text{OH})_4]$

Ms. 2: synthetic muscovite. $T = 775$ K; $P_{\text{H}_2\text{O}} = 10^8$ Pa; $t = 148$ h; stoichiometric mixture: $\text{KCl} + \gamma\text{-Al}_2\text{O}_3 + \text{SiO}_2$

Ma.: synthetic margarite. $T = 723$ K; $P_{\text{H}_2\text{O}} = 2 \times 10^8$ Pa; $t = 240$ h; stoichiometric mixture: $\text{CaSO}_4 \cdot 2\text{H}_2\text{O} + \gamma\text{-Al}_2\text{O}_3 + \text{SiO}_2$

(II) Natural specimens

Ch. 1: metamorphic chlorite from Piedmont (Italy)

Ch. 2: natural chlorite from a fine-grained phyllite of 'Piedmont belt', Coast Range, Venezuela

Ch. 3: detrital-(metamorphic)-chlorite from black shales of the Eboinda region, Ivory Coast

B.: metamorphic biotite from gneisses of Bormes, Maures Massif, Var, France

To illustrate this, we discuss here a few of the more common or more interesting types of defects induced by growth and deformation phenomena in phyllosilicate minerals which are particularly rich in structural heterogeneities as already observed using HRTEM (Amouric & Baronnet, 1983; Amouric, Baronnet & Finck, 1978). These defects mainly consist of linear and planar defects with or without chemical perturbations (intercalations) in the structures concerned.

2. Experimental and specimens

Experimental HRTEM images of synthetic and natural phyllosilicates were recorded. Synthetic muscovites, margarite and phengite were produced from a stoichiometric mixture of the mica components through spontaneous nucleation of the mica under hydrothermal conditions (see Table 1). The origins of the natural specimens studied (chlorites and biotites) are very different and are also specified in Table 1. Because HRTEM requires a minimum specimen thickness (<150 Å) parallel to the electron beam, phyllosilicate slices were prepared by means of ultramicrotoming and ion-thinning techniques following the procedures detailed elsewhere by Amouric & Parron (1985).

A conventional JEM 100C electron microscope, equipped with an objective lens pole piece with a spherical coefficient $C_s \approx 1.7$ mm, was used in this

study. All micrographs were recorded in bright-field illumination. Reflections passing through a $40\ \mu\text{m}$ objective aperture centered on the incident beam at 100 kV contributed to the image. The point-to-point resolution was therefore constrained to $\geq 3\ \text{\AA}$. Images were selected from an experimental through-focus series recorded in the 800–1200 \AA range of under-focusing. These best imaging conditions for phyllosilicates were defined by referring to previous image simulation in micas (Amouric, Mercuriot & Baronnet, 1981). Observation parallel to the phyllosilicate layers, particularly useful in the structural analysis of micas (Amouric, Baronnet & Finck, 1978; Amouric & Baronnet, 1983) was thus made.

3. Growth defects

The linear and planar growth defects which generally involve no chemical change in the structures are first distinguished. The linear defects are called 'dislocations'. Edge and screw dislocations are the two main types. So, for example, if 'an additional half-plane' is inserted between two consecutive planes in a mica structure, we obtain the configuration of an edge dislocation as shown in Fig. 1 for a synthetic phengite (Ph., Table 1). The boundary of the additional half-plane inside the crystal is the dislocation line. In Fig. 1, a triangular bright contrast (arrowed) reveals the core of the dislocation. Around the dislocation line, we can observe a bending of mica sheets which progressively diminishes when going away from the core of the dislocation. The Burgers vector, in this case, is equal to $10\ \text{\AA}$ and is normal to (001). Such a bending generally permits an evaluation of the elastic deformation due to the defect. Dislocation cores (edge and screw) are very important structural anomalies because they form real 'channels' running along the dislocation lines. Through these 'channels', diffusion phenomena and chemical exchange are much easier for the crystal than through its normal structure. Dislocation cores also favour the mobility of dislocations. In particular, if edge dislocations are not operative in the crystal growth mechanisms, their possible movement is fundamental in the plastic deformation phenomena of crystals.

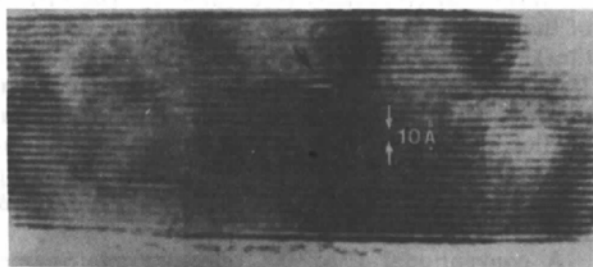


Fig. 1. 00l lattice-fringe image of a synthetic phengite with an edge dislocation (black arrow).

Near a screw dislocation, the planes of atoms form a helix around the dislocation line and may give a well known growth spiral as observed at the surface of many minerals (Dekeyser & Amelinckx, 1955; Baronnet, Amouric & Chabot, 1976). Such dislocations are primordial for the crystal growth when the energy of the growth system is low (Burton, Cabrera & Frank, 1951). In micas, the building up of 'basic structures' is most probably related to the very early stages of crystal growth (Amouric & Baronnet, 1983), *i.e.* three-dimensional nucleation, followed by the layer-by-layer growth of the basal faces. Subsequent growth by spirals allows further development of the basic structures under low supersaturation rates, and to a much lesser extent, the generation of new complex superstructures when the Burgers-vector components along c^* are non-integral multiples of the basic structure-repeat distance. Fig. 2 indirectly illustrates this last case in a synthetic muscovite (Ms. 1, Table 1). The 00l lattice-fringe image reveals (Fig. 2a) a $40\ \text{\AA}$ superperiodicity, repeated four times along c^* . On the left of the crystallite, successive $40\ \text{\AA}$ steps (arrowed) coincide with the superperiodicity. So, HRTEM shows a complex mica polytype generated by spiral growth certainly around a screw dislocation having a $40\ \text{\AA}$ exposed ledge and a dislocation line perpendicular to the layers (Fig. 2b). The $10\ \text{\AA}$ periodicity of the basic crystallite is not significant, but the $30\ \text{\AA}$ sequence locally observed on the right of Fig. 2(a) suggests that the basic structure of this muscovite is a $3T$ or a faulted $2M_1$ one.

As in Fig. 2, dislocations and planar defects are often observed together, related to growth phenomena. Assuming that the only permitted stacking

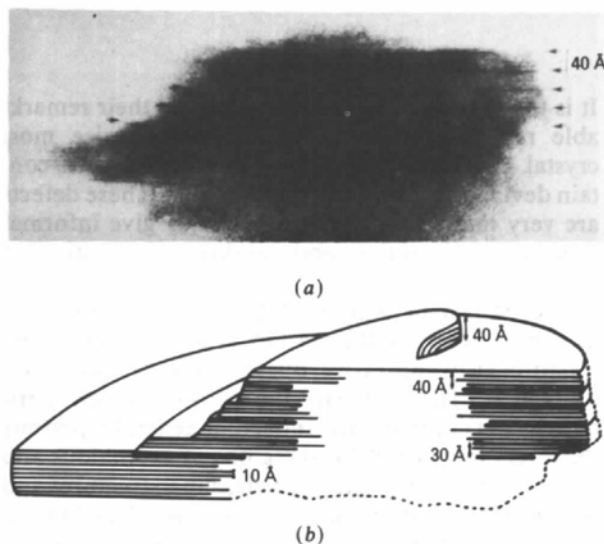
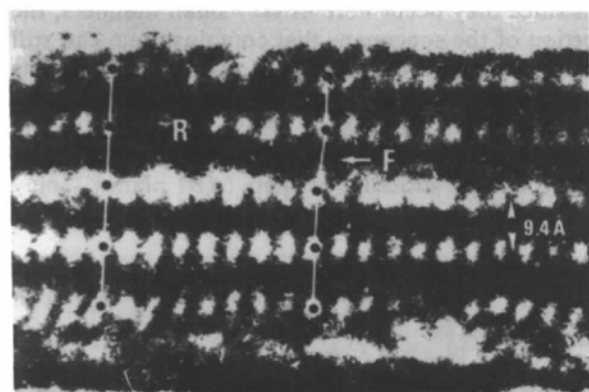
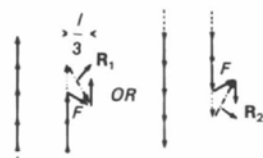


Fig. 2. (a) 00l lattice-fringe image of a synthetic muscovite with a $40\ \text{\AA}$ superperiodicity (arrows). Note the $40\ \text{\AA}$ steps on the left. (b) Analytical diagram of (a). The superperiodicity is generated by a spiral growth mechanism due, itself, to screw-dislocation activity.

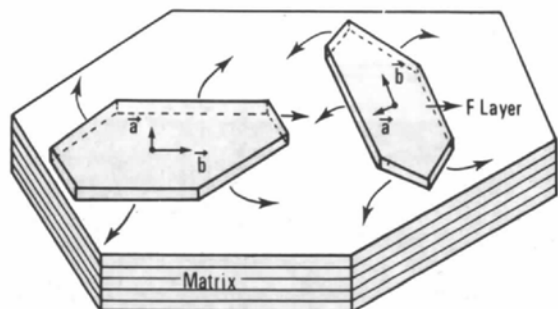
angles between mica layers are 0 or $\pm 120^\circ$ and under very drastic observation conditions, the intimate stacking sequences of layers within individual mica crystallites may be determined by structure-imaging techniques with HRTEM (Amouric & Baronnet, 1983; Amouric *et al.*, 1978, 1981; Iijima & Buseck, 1978). Fig. 3 is a structure image of a very small synthetic margarite (Ma., Table 1) viewed along $[\bar{1}00]$. On the left part of the micrograph, the sequence of the white dots along c^* is regular revealing a pure $1M$ polytype (with successive 0° stacking angles between the layers); but on the right part, the upper white dots of the F layer are abnormally shifted to the right. This characteristic shift means (Amouric & Baronnet, 1983) that there is a $\pm 120^\circ$ rotation of the F layer and therefore a 'partial' stacking fault (F) at



(a)



(b)



(c)

Fig. 3. (a) Structure image of a $1M$ synthetic margarite viewed along $[\bar{1}00]$. A stacking fault (F) is limited by a partial dislocation (R). (b) The two possible corresponding stacking sequences as shown by their (Smith and Yoder) stacking vector representation. (c) Analytical diagram of (a).

this level in the sequence. Since the contrast of the white dots is very weak in the R zone (Fig. 3a) which limits the stacking fault (F), the R zone certainly marks the location of a partial dislocation line, the fault vector of which is $R_{1,2} = \frac{1}{3}[3\bar{1}0]$ (Fig. 3b). The layer-by-layer growth mechanism in micas allows the occurrence of such a partial dislocation in a perfect matrix to be explained. For this, we have to consider that the right and left parts of the F level in the crystallite have independently nucleated on the same support, each with a different stacking vector (Fig. 3c). Then the partial dislocation was formed at the junction of the two bidimensional nuclei, during their lateral development.

The main known planar defects are stacking faults. As seen in Fig. 3, they change the regular stacking of the structural elements when passing through planar surfaces and commonly produce 'twin' configurations, mainly in compact and lamellar structures. The frequency of stacking faults, in a single crystal, is variable. When they are numerous, the stacking faults may be perfectly repeated so that the crystal stays strictly periodic but shows a superperiodicity perpendicular to the fault planes, giving a superstructure such as the complex mica polytype shown in Fig. 2.

Sometimes also, the distribution of stacking faults in one crystal is irregular and even completely at random. The resulting crystal may be ordered parallel to the fault planes and completely disordered perpendicular to these planes (one-dimensional disorder). Here still, such a structure can be finely resolved and directly imaged with HRTEM, which is impossible with X-rays which give only an average and statistical idea of a structural disorder. Fig. 4 is a bidimensional image of a natural chlorite (Ch. 1, Table 1) showing dark fringes separated by rows of white spots. The wider fringes correspond to the talc-like layers (T) and the narrower ones correspond to the brucite-like layers (B) of the chlorite structure. T and B layers alternate regularly without exception. If we note respectively (+) and (-) the right and left shifts of the successive T and B layers along c^* , the observed stacking sequence of this chlorite is the following: $B_+T_-B_+T_+B_0T_0B_0T_+B_-T_-B_-T_-B_+T_-B_-T_-B_-T_-B_-T_0B_0T_-B_-T_+B_0T_+B_-T_-B_-T_+B_+T_-B_0T_+B_0T_-B_+$. So the shifts across the T layers, as those across the B layers, both vary with no apparent pattern. Spinnler, Self, Iijima & Buseck (1984) have shown an HRTEM micrograph of a chlorite where the talc staggers in the stacking sequence all have the same sign (T_+) whereas the brucite staggers vary, and they have concluded that this kind of disorder observed in their chlorite could be explained in terms of 'semi-random' stacking as termed by Brown & Bailey (1962) who considered it to be common. This is not the case in Fig. 4, except perhaps on four or five layers where the talc staggers are successively T_- . So we can

conclude that Fig. 4 illustrates – and for the first time – a ‘complete-random’ chlorite-stacking sequence.

From bidimensional images it is also possible to distinguish different kinds of stacking faults in the same mineral species as illustrated by our HRTEM observations of nucleation experiments on OH-muscovite (Amouric & Baronnet, 1983) (Ms. 2, Table 1). In Fig. 5, the entire stacking sequence of this small crystallite can be unravelled. From the ‘white dots’ sequence, the structure may be considered as $1M$ with a faulted layer F ($\pm 120^\circ$ rotation) inserted between the two upper layers. The resulting fault is of the extrinsic type. It may be symbolized by E_0^{22} ($1M$) and considered as a low-energy fault according to the mica-fault theory and notations of Baronnet, Pandey & Krishna (1981). In the same manner, a twice-faulted $2M_1$ sequence occurs in the seven-layered crystallite shown in Fig. 6. The faulted layer F_2 seems to create a low-energy intrinsic fault of type I_2^0 ($2M_1$) (Baronnet *et al.*, 1981). Such observations give direct evidence of the early genesis of mica basic structures more or less altered by growth faults. In this respect, HRTEM, applied to micas nucleating under known conditions, is a very powerful tool for determining the factors which govern the growth of a selected basic structure and its state of order. Furthermore, the proof of the existence of selected basic structures containing a single low-energy growth fault near the surface, at the time the screw dislocations originate, allows us to explain directly, with the faulted-matrix model of Baronnet *et al.* (1981), most of the 23 known complex polytypes of the micas (Baronnet & Amouric, 1983).

While the various linear and planar structural defects described above do not alter the chemical composition of the crystal matrix, this is not the case

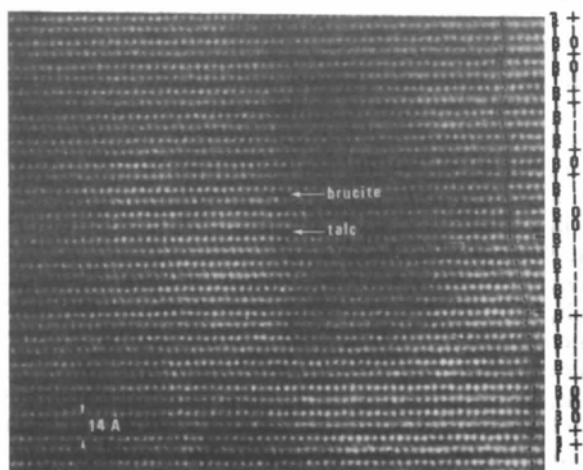


Fig. 4. Structure image of a natural chlorite with talc-like layers (T) and brucite-like layers (B) regularly alternating. Black bars show the completely disordered stacking sequence of this chlorite along c^* .

for the so-called ‘intercalation’ growth defects which occur as intergrowth phenomena and which are still planar defects. These latter imply, in the matrix sequence, the stacking of structural units with a distinct (but related) architecture and a distinct chemical composition. However, these intercalations show a great structural analogy with the matrix in their planar contact and thus usually exhibit coherent interfaces. Fig. 7 shows two simple examples of such intergrowths within a natural chlorite structure (Ch. 2, Table 1), with extra brucite-like layers (Fig. 7a) resulting in planes with adjacent brucite layers (these defects could be alternatively described as missing talc-layers) and extra talc-like layers (or missing brucite-like layers) (Fig. 7b). Chemically, these defects represent silica-poor, hydroxyl-rich layers (Fig. 7a) and relatively silica-rich zones (Fig. 7b), but since they occur here in very small numbers, the portion of the specimens that contains them can still be considered to be chlorite. However, such defects – commonly observed with HRTEM in sheet-silicate clay minerals (see Veblen, 1983; Buseck, Nord & Veblen 1980; Olivès Banos, 1985) because they have a very similar structure in their (a,b) planes – may

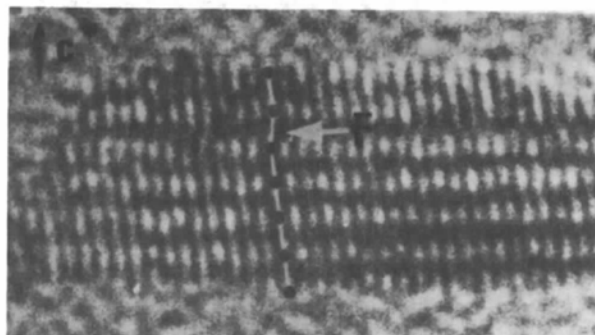


Fig. 5. Structure image of a synthetic muscovite with a $1M$ structure viewed along $[110]$ or $[\bar{1}\bar{1}0]$. The single layer marked F (arrowed) corresponds to an extrinsic stacking fault in the $1M$ sequence.

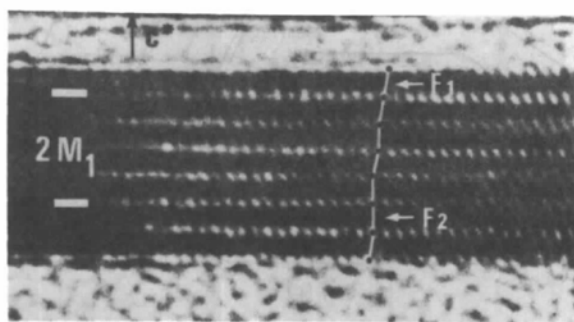


Fig. 6. Structure image of a synthetic muscovite with a twice-faulted $2M_1$ structure viewed along $[\bar{1}\bar{1}0]$ or $[110]$. The layer marked F_2 corresponds to an intrinsic stacking fault in the $2M_1$ sequence.

also occur in other mineral groups such as oxides (see, for example, Mellini, Amouric, Baronnet & Mercuriot, 1981). A very important problem arises concerning the interpretation of classical microprobe analytical results of such faulted minerals, because the resulting mixed layering affects both stoichiometry and apparent cation-partitioning trends (Veblen, 1983). Furthermore, it can be difficult to recognize intercalation defects in powder X-ray diffraction patterns. This strongly suggests that the only way to carefully study intergrowths of different structural units consists of combining HRTEM observations with X-ray microanalysis techniques.

4. Deformation defects

There are practically no published HRTEM studies on the deformation of phyllosilicates. However, HRTEM may also be a powerful tool for exploring

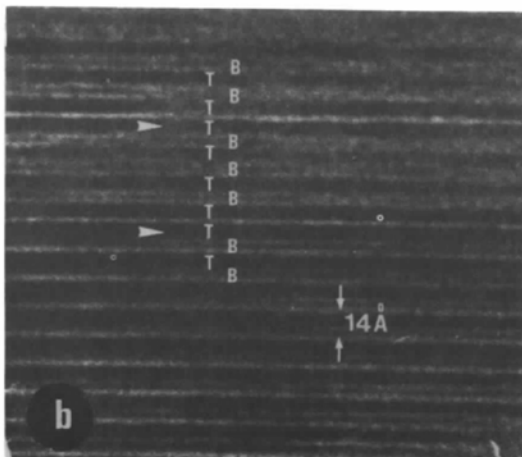
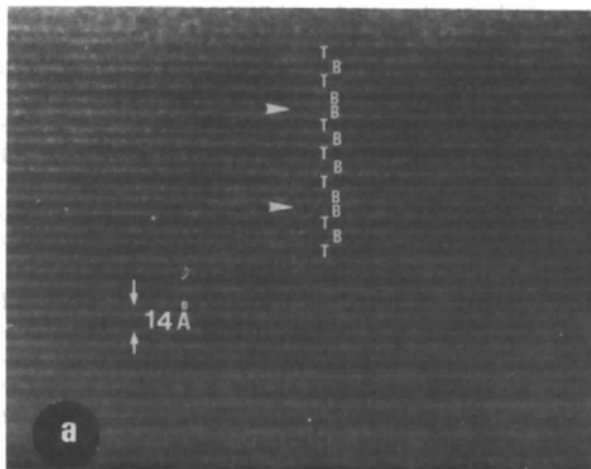


Fig. 7. One-dimensional image showing fine-scale intergrowths of (a) extra brucite-like layers and (b) extra talc-like layers within a chlorite-type structure.

the relevant mechanisms related to mineral deformation and for reconstructing their tectonic history. The presence, in phyllosilicates, of only one slip plane parallel to the (001) cleavage plane is responsible for their characteristic modes of deformation involving basal slips, basal (micro)cleavages, bending and kinking, the two first modes corresponding to the main mechanisms. The important question about the exact location of such deformation defects - on the scale of interatomic distances - was first solved by our HRTEM observations of metamorphic biotites (Olivès Banos, Amouric, De Fouquet & Baronnet, 1983). For example Fig. 8 shows a simple microcleavage of unsymmetric shape which was unambiguously produced by a basal slip in a biotite (B., Table 1) subjected to a metamorphic stress probably parallel to its (001) planes. This image clearly reveals that slip has occurred in the same atomic plane as cleavage, that is in the interlayer level characterized by a very low density of atoms (bright fringes in Fig. 8), as previously explained by Olivès Banos & Amouric (1984).

Various states of deformation can be attained. In Fig. 9, triangular-shaped basal microcleavages are visible, aligned along the axial plane of a fold in a chlorite (Ch. 3, Table 1). This configuration allows a discontinuous increase of the radius of curvature of basal planes in the hinge zone of the fold, from the outer (with respect to the fold) sides to the inner sides of the cleavages and, in this way, the chlorite accommodates the compressive stress.

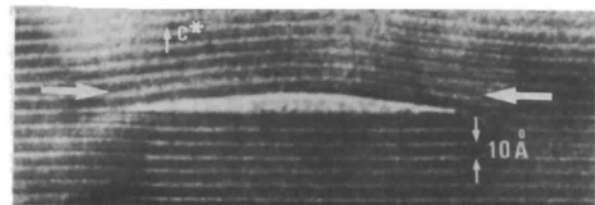


Fig. 8. 001 lattice-fringe image of a metamorphic biotite showing a microcleavage produced by basal slip in the interlayer level.

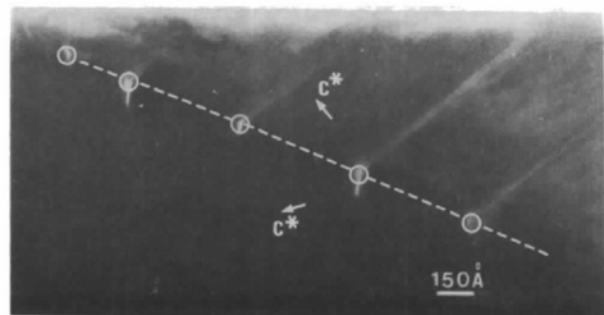


Fig. 9. One-dimensional image of a folded natural chlorite. Note the triangular basal microcleavages (O) along the axial plane of the fold.

Normally, slip phenomena are favoured when the maximum compressive stress is at about 45° to the (001) slip plane in phyllosilicates (Schneider, 1978). However, it is relatively easy to deform these minerals at a small angle to (001). In this case, the deformation is heterogeneous and achieved by basal slip associated with bending and kinking (Etheridge, Hobbs & Patterson, 1973; Olivès Banos, private communication). Fig. 10 illustrates this and shows a one-dimensional image of a kink in a natural chlorite (Ch. 1, Table 1) with talc-like layers (wider fringes) and brucite-like layers (narrower fringes) visible. We note that the folding is perfectly polygonized for the zones in compression and rounded for the stretched zones (the inner and outer parts of the fold, respectively). Structural blocks, turned relative to their initial position, are separated by different joints [the main being the kink band boundary (KBB)], which permit such a deformation. So the folding of the structure is realized over a very short distance. Furthermore, owing to the deformation, a crack (triangular microcleavage) is opened at the base of the KBB. This means a flow of solutions may take place through such a porosity and allow the mass transfers required for the metamorphic transformations, even inside single crystals.

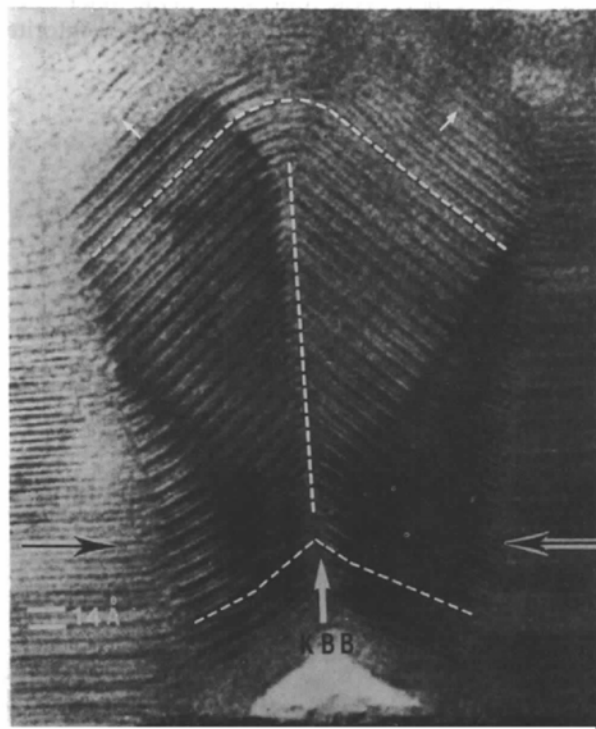


Fig. 10. One-dimensional image of a kink in a natural chlorite. Note the polygonized and the rounded zones marking respectively the inner and the outer part of the fold and a triangular microcleavage at the base of the KBB (kink band boundary).

Revealing a high degree of deformation, the mechanisms described above, with their characteristic structural defects, may occur together and act strongly in phyllosilicates. For example Fig. 11 shows a chlorite (Ch. 3, Table 1) exhibiting chevron-type folds. In this image, the parallel basal planes of chlorite diverge quasi-periodically in opposite directions through successive folding joints, with a 40–70 Å wavelength. As a general rule, by studying such deformation defects in natural minerals with HRTEM, it should be possible to determine with good accuracy the direction of the maximum stress which has operated on the host rocks.

Related to deformation phenomena such as slips and microcleavages, some intercalation defects revealed by HRTEM may be regarded as 'secondary' (indirect) deformation defects. This type of intercalation, which also changes the chemical composition of the crystal matrix, is genetically posterior to the growth of the crystal matrix. Such secondary deformation defects have been observed by us in metamorphic biotites (B., Table 1) (Olivès Banos *et al.*, 1983, Olivès Banos & Amouric, 1984) giving rise to various interlayered mica-chlorite structures. For example in Fig. 12(a), the biotite-chlorite layer sequence imaged is disordered (which is the general case) but in the lower part of Fig. 12(b), it appears as an ordered 1/1 sequence. Furthermore, lateral transitions of a unit biotite layer into a unit chlorite layer were also frequently observed in the same specimen (Olivès Banos *et al.*, 1983; Olivès Banos & Amouric, 1984). They always occurred as transitions of a plane of potassium ions into a brucite-like layer. In such a context, we have interpreted these chlorite intercalations as a 'brucitization' of interlayer levels of the primary metamorphic biotites where partial slips or cleavages have previously occurred. In this way,

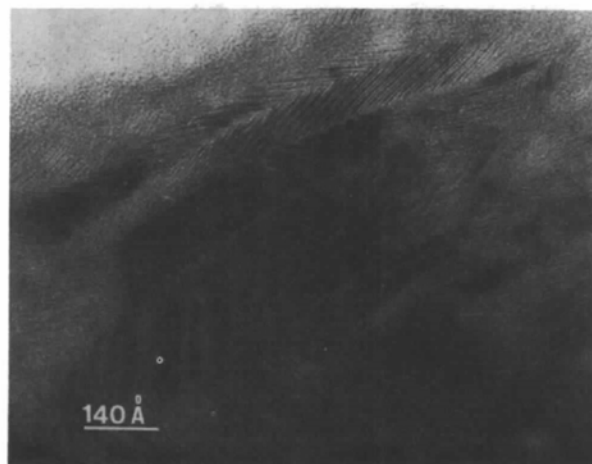


Fig. 11. One-dimensional image of a chevron-type fold in a natural chlorite.

HRTEM shows an example of a chemical process at the atomic level, favoured by deformation microstructures.

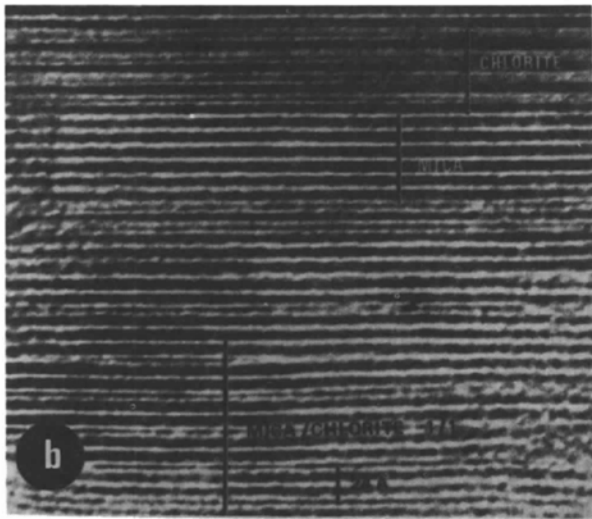
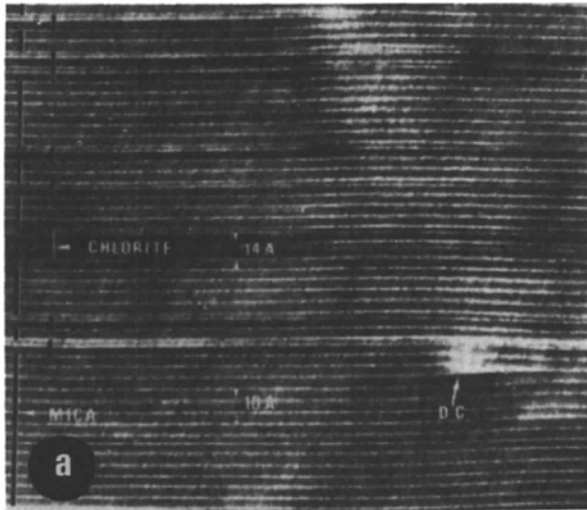


Fig. 12. One-dimensional images of interlayered biotite-chlorite structures. The biotite-chlorite layer sequence is (a) disordered and (b) ordered (1/1) (lower part).

5. Conclusion

HRTEM is today an unrivalled method for studying the intimate structure of crystals and particularly their defects. Since most minerals are faulted, its applications may cover a wide range of structural anomalies. Among them, the linear and planar defects - which are generally the most readily seen defects (Buseck & Veblen, 1981) - play an important role during growth and deformation phenomena in phyllosilicates. We have to bear in mind however that, while it demonstrates the possible structural and chemical complexities of minerals, HRTEM may somewhat perturb our concept of phase and solid solution.

References

- AMOURIC, M. & BARONNET, A. (1983). *Phys. Chem. Miner.* **9**, 146-159.
- AMOURIC, M., BARONNET, A. & FINCK, C. (1978). *Mater. Res. Bull.* **13**, 627-634.
- AMOURIC, M., MERCURIOT, G. & BARONNET, A. (1981). *Bull. Mineral.* **104**, 298-313.
- AMOURIC, M. & PARRON, C. (1985). *Clays Clay Miner.* **33**, 473-482.
- BARONNET, A. & AMOURIC, M. (1983). *Proceedings of the 41st Annual Meeting of the Electron Microscopy Society of America*, edited by G. W. BAILEY, pp. 174-177. San Francisco Press.
- BARONNET, A., AMOURIC, M. & CHABOT, B. (1976). *J. Cryst. Growth* **32**, 37-59.
- BARONNET, A., PANDEY, D. & KRISHNA, P. (1981). *J. Cryst. Growth* **52**, 963-968.
- BROWN, B. E. & BAILEY, S. W. (1962). *Am. Mineral.* **47**, 819-851.
- BURTON, W. K., CABRERA, N. & FRANK, F. C. (1951). *Philos. Trans. R. Soc.* **243**, 299-358.
- BUSECK, P. R., NORD, G. L. & VEBLEN, D. R. (1980). In *Pyroxènes*, edited by C. T. PREWITT, pp. 117-121. Mineralogical Society of America.
- BUSECK, P. R. & VEBLEN, D. R. (1981). *Bull. Mineral.* **104**, 249-260.
- DEKEYSER, W. & AMELINCKX, S. (1955). *Les dislocations et la croissance des cristaux*. Paris: Masson.
- ETHERIDGE, M. A., HOBBS, B. E. & PATTERSON, M. S. (1973). *Contrib. Mineral. Petrol.* **38**, 21-36.
- IJIMA, S. & BUSECK, P. (1978). *Acta Cryst.* **A34**, 709-719.
- MELLINI, M., AMOURIC, M., BARONNET, A. & MERCURIOT, G. (1981). *Am. Mineral.* **66**, 1073-1079.
- OLIVÈS BANOS, J. (1985). *Bull. Mineral.* **108**, 635-641.
- OLIVÈS BANOS, J. & AMOURIC, M. (1984). *Am. Mineral.* **69**, 869-871.
- OLIVÈS BANOS, J., AMOURIC, M., DE FOUQUET, C. & BARONNET, A. (1983). *Am. Mineral.* **68**, 754-758.
- SCHNEIDER, H. (1978). *Mineral. Mag.* **42**, 41-44.
- SPINNLER, G. E., SELF, P. G., IJIMA, S. & BUSECK, P. R. (1984). *Am. Mineral.* **69**, 252-263.
- VEBLEN, D. R. (1983). *Am. Mineral.* **68**, 566-580.